Supporting Information

Tang et al. 10.1073/pnas.1007591107

SI Materials and Methods

Sequence Analyses. The homologous sequences of *Dm310s* in *D. sechellia*, *D. simulans*, *D. yakua*, *D. erecta*, *D. ananassae*, and *D. pseudoobscura* were parsed from the whole-genome alignments of the 12 *Drosophila* species (http://genome.ucsc.edu). Phylogenetic reconstruction among the mature sequences of *miR310s* was done with the neighbor-joining method (1) based on Kimura's two-parameter distances (2) as implemented in MEGA version 4.0 (3).

Cloning and Transformation. Five hundred sixty-one base pairs containing four miRNAs of *miR310s* were amplified from D. melanogaster line Iso-1 genomic DNA utilizing PCR with Platinum Taq HiFi (Invitrogen), using the following primer pair with 5′ restriction sites: mel-310-F (5′-CGGAATTCGTATTACCCGACATCGTTCTAGCC-3′) and mel-310-R (5′-CCCTCGAGCGATTTCACAGATTTAAATGTTGA-3′); the homologous cluster in *D. pseudoobscura* was amplified from genomic DNA of a WT strain using the primer pair, pse-310-F (5′-GAGAATTCAGTGCGTGCAGTGGAACTGAAAAT-3′) and pse-310-R (5′-GACTCGAGAGGCCGAAGACTGCCAATATGTTA-3′). Cycling conditions were 95 °C for 3 min, followed by 30 cycles at 95 °C for 30 s, 55 °C for 30 s, and 68 °C for 1 min, and then 68 °C for 7 min. The amplicon was gel-purified, restriction-digested, and cloned into the EcoRI and XhoI sites of pUAST (4). Before using the cloned DNA for transforming flies, the clone was sequenced to verify that there were no errors during amplification. w1118 flies were transformed with p(*UAS-Dm310s*) or p(*UAS-Dp310s*), using pTURBO (Flybase. ID:FBmc0002087) helper plasmid and standard procedures (5).

Fly Stocks. We used the *P{GawB}* line NP5941 (Kyoto Stock Center; no. 113798) as a source of GAL4. The P-element in this line is inserted 173 bp upstream from stem-loop *miR-313*, the first miRNA in *miR310s*. NP5941 flies themselves are extremely healthy and are phenotypically WT. Other GAL4 stocks used were *P{GawB}DJ715* (Bloomington Stock Center; no. 8179) and *P{Act5C-GAL4}25FO1* (Bloomington Stock Center; no. 4414). EP(2)2587 [*P(3)l(2)05510EP2587*; Szeged Stock Center)] was used for the imprecise excision screen to produce the *Dm310s* knockout. All stocks were maintained on yeast-cornmeal agar at 25 °C on a 12-h light/dark cycle.

Generation of *Dm310s* Deletion. The *Dm310s* null allele was generated in an imprecise P-element excision screen using the stock EP(2)2587 that contains a P-element inserted 76 bp upstream of the 5′ end of *miR-313* EST (6). Of the four miRNAs in *Dm310s*, *miR-313* is the closest downstream of the EP(2)2587. The P element in EP(2)2587 was mobilized with Δ2–3 transposase from a stable Δ2–3 chromosomal insertion at cytological position 99B. White-eyed male progeny were crossed to a CyO balancer strain and analyzed by PCR analysis using primers corresponding to the P element and/or the genomic sequences flanking it. PCR sequencing identified a 1,416-bp deletion removing the whole *miR310s* cluster with the flanking genes intact.

Viability Assay. Ten balanced female flies from each transformant line were crossed with 10 GAL4 homozygote male flies in three independent experiments. Two kinds of GAL4 lines, DJ715 and NP5941, were used for the viability assay. Parent flies were transferred to fresh vials after 3 d of egg-laying, thereby providing us with six vials' worth of progeny from each cross. The balanced female flies carrying the UAS transgene provided an internal control of the fertility of the female flies. The number of progeny with or without balancer was scored for each kind of cross. Viability was calculated as the number of progeny carrying the balancer against the number of UAS-GAL4–containing progeny. The viability assay using the *NP5941-GAL4* line was repeated twice independently. The Kolmogorov–Smirnov test and Mood's median test detected no significant difference ($P > 0.05$) in the distribution of viability among transgenic lines. We therefore pooled the data together to calculate the viability of each transgenic line when driven by NP5941-GAL4. A bar plot was used to display the frequency of *Dm310s* and *Dp310s* transgenic lines with different viability effects when they were driven by GAL4 line DJ715 or NP5941. Mann–Whitney *U* tests were used to test the viability difference between *Dm310s* and *Dp310s* lines. The correlation of viability under the control of two kinds of GAL4 was determined using the Spearman rank correlation test.

Northern Blot Hybridization. Using *NP5941-GAL4* virgin female flies and *UAS-miR310s* male flies (in which the 310 cluster is derived from either *D. melanogaster* or *D. pseudoobscura*), crosses were set up in vials on cornmeal agar at 25 °C with a 12-h light/dark cycle. That *miR310s* was, in fact, being overexpressed was tested using a small RNA Northern blot protocol. Briefly, L3 progeny larvae were collected and RNA was extracted using the miRvana RNA extraction kit (Ambion, Inc.). Thirty micrograms of small RNA was loaded in each well of a 15% (wt/vol) urea-PAGE assay and run at 4 °C for about 2 h. The RNA was transferred to a positively charged nylon membrane (Roche Diagnostics) using a semidry transfer apparatus (Fisher Scientific). RNA was fixed using UV cross-linking (Hoefer) and was probed using digoxigenin-labeled (Roche Applied Science) antisense DNA probes (IDT) to one miRNA in either the *D. melanogaster* (miR-312) or *D. pseudoobscura* (second miRNA encoded by the cluster) 310 cluster at 48 °C overnight in UltraHybe-oligo buffer (Ambion, Inc.). After developing blots, membranes were stripped according to manufacturer protocols and reprobed with a DNA probe to detect the 30-nt 2S rRNA. Probe sequences were anti-Dme-miR-312 (5′-TCAGGCCGTCTCAAGTGCAATA-3′), anti-Dps-miR-312 (5′-TTGGACCGGGGCTAGTGCAATA-3′), and anti-2S rRNA (5′-TACAACCCTCAACCATATGTAGTCCAAGCA-3′). Alkaline phosphatase-tagged antibody (Roche Diagnostics) was used to probe the DIG-labeled RNA probe further, and the membrane was developed using a CDP-Star kit (Roche Applied Science).

Semiquantitative RT-PCR. Progeny L3 larvae were collected from the crosses between NP5941 female and male flies from w1118, *Dm310s*, and *Dp310s* lines. Total RNA was extracted using the miRvana RNA extraction kit. The expression levels of *miR310s* were quantified with end-point stem-loop RT-PCR (7). Pilot experiments were performed initially to make sure that only single specific products were obtained with the PCR primers and to determine the amount of RT product dilution and the range of cycle number to use. Briefly, 50 ng of total RNA was reverse-transcribed with miR-specific stem-loop primer using a Taqman MicroRNA Reverse Transcription Kit (Applied Biosystems) following the manufacturer's instructions, except that the reaction volume was scaled down to 7.5 μL. One microliter of RT product was subsequently used as a template for the RT-PCR amplification in a 10-μL reaction system of Taqman Universal PCR Master Mix (Applied Biosystems). The PCR cycling conditions were as follows: 95 °C for 15 min for the initial activation step, with 35 cycles each of 94 °C for 15 s, 60 °C for 30 s, and 72 °C for 20 s. 2S rRNA was used as

a control gene. The RT product of 2S rRNA was diluted 1,500-fold, and 1 μL was added as template in a 10-μL PCR system. Primers used are listed in Table S1. Amplicons were visualized on a 3% (wt/vol) TAE agarose gel. Images were analyzed using a Gel-Pro Analyzer 4.0 (Media Cybernetics, L.P.). The whole assay was done with three biological repeats.

Microarray Assay. To detect the effect of cross-species *miR310s* on the transcriptome, we collected L3 progeny larvae from the crosses between NP5941 female and *UAS-miR310s* male flies; L3 larvae from the cross between NP5941 female and w1118 male flies were used as controls. Total RNA was extracted using TRIzolR Reagent (GIBCO BRL), followed by purification with an RNeasy Mini kit (QIAGEN). Microarray assays were performed on two different platforms: DGRC-1 Amplicon Transcriptome Microarrays (Drosophila Genomics Resource Center, Indiana University, Bloomington, IN) and Drosophila Tiling 1.0F Arrays (Affymetrix).

Dm310s line M1–7 and *Dp310s* line P4–18 with median viability among either *Dm310s* or *Dp310s* lines were used in the crosses for cDNA microarray analysis. After RNA extraction and purification, cDNA synthesis, hybridization, and washing were performed according to the Dendrimer Use and Hybridization Protocol from the Drosophila Genomics Resource Center (8). Six cDNA microarrays in three dye-swap pairs were used, with each pair comparing either control and transgenic line or two types of transgenic lines. Slides were scanned using a GenePix 4000B microarray scanner (Axon Instruments). Cy3 and Cy5 intensities of cDNA microarrays were extracted using GenePix Pro. 6 (Axon Instruments).

In addition to the two transgenic lines used in the cDNA microarray, a more viable *Dm310s* line, M1–3, was included in the crosses for the tiling arrays to validate the consistency of results in the consideration of position effect. Triple biological repeats were conducted for each sample, resulting in 12 tiling arrays in total. The expression profiles of the imprecise and precise deletions of EP(2)2587 were also compared by using 6 tiling arrays with triple biological repeats for each genotype. Total RNA was extracted from L3 larvae as described above. Double-stranded cDNAs were reverse-transcribed from total RNA samples with the One-Cycle cDNA Synthesis Kit (Affymetrix) in the presence of oligo (dT)20 primer (Invitrogen). The cDNA was purified by means of a GeneChip Sample Cleanup Module (Affymetrix) and then biotin-labeled using a BioPrime DNA labeling system (Invitrogen). Hybridization, washing, staining, and scanning were carried out following the GeneChip Whole Transcript Double-Stranded Target Assay Manual (Affymetrix). The hybridized *Drosophila* tiling 1.0F arrays were scanned using a GeneChip Scanner 3000 (Affymetrix). Raw data of tiling arrays were collected by means of Affymetrix GeneChip Operating software.

Microarray Analyses. Raw data from cDNA arrays were normalized using within-array print-tip locally weighted scatterplot smoothing (LOESS) normalization and between-array quantile normalization as implemented in the BioConductor package Linear Models for Microarray Data (LIMMA) (9). Differential gene expression was determined using a linear modeling approach, followed by empirical Bayes moderated *t* statistics (10). The design matrix was constructed for directed two-color design without common reference so that the coefficients estimated by the linear model correspond to the $\log_2$ ratios of *Dm310s* line M1–7 vs. control and *Dp310s* line P4–18 vs. control. Moderated *t* statistics were used to evaluate differential expression between each pair of contrasts. Intensities of null and control spots were discarded before fitting the linear model. The *P* values generated by this analysis were adjusted to control the false discovery rate (FDR) using the Benjamini–Hochberg method (11).

Quantile normalization was applied to the Probe Cell intensity file (the CEL file) of the 12 tiling arrays of the *Dm310s*(+) set and 6 tiling arrays of the *Dm310s*(−) set using CisGenome (http://www.biostat.jhsph.edu/~hji/cisgenome/), where outlier and masked cells were removed in the CEL files. The probe sequences of the *Drosophila* tiling 1.0F array (Affymetrix) were mapped to *D. melanogaster* genome and transcript datasets release 5.4 (ftp://ftp.flybase.net/genomes/Drosophila_melanogaster/dmel_r5.4_FB2007_03) using the BLAST-like alignment tool (BLAT) (12). The perfect-match 25-bp probes that have a single hit to the genome and are specific to the transcripts of a single gene were used for expression analysis. For the annotated transcripts with more than three probes, a paired *t* test was applied to the mean intensity of each probe within a transcript-specific probe set to determine the differential expression between the genotype of interest vs. control. *P* values were adjusted for multiple testing using the Benjamini–Hochberg method (11). For both cDNA and tiling arrays, transcripts that changed at least 1.5-fold with respect to the control having a significant threshold of FDR = 0.05 were considered as differentially expressed. The expression fold changes for tiling arrays were calculated using the mean intensity of the probe set. All the microarray data have been deposited in the Gene Expression Omnibus (GEO) under the SuperSeries accession number GSE15863.

Volcano plots were used to display the significance of expression difference against $\log_2$-fold changes. Empirical cumulative plots were used to visualize the difference in $\log_2$-fold change distribution between the WGE transcriptome and the subset of putative targets of *miR310s*. In empirical cumulative plots, we used only a single transcript that has miRNA target prediction on its 3′UTR [from the TargetScan Web site (http://www.targetscan.org)] to present each gene, calculated as the median fold change of these transcripts for the *Dm310s*, *Dp310s*, and *Dm310s*(−) lines, and then centered the fold change distribution of the reported genes having target prediction to zero by subtracting the median from the fold changes for each line. The above analyses were performed with the R package (http://www.R-project.org) (13).

Target Prediction. Target predictions from TargetScan release 5.1 (14, 15), PicTar (single miRNA target predictions with the setting S1) (16), and PITA "TOP" category with 3/15 flank version 6 (17) were obtained from the respective Web sites. We further separated the evolutionarily conserved and unconserved targets and focused on those with perfect-match 3′UTR sites to positions 2–8 of miR (denoted as 8-mer sites in this study). The 3′UTR alignments of 12 *Drosophila* species were downloaded from the TargetScan Web site (http://www.targetscan.org). The conserved and nonconserved targets with 8-mer sites were predicted using the TargetScanS algorithm (14), where 8-mer sites in this study are equal to the "8mer" (the Watson–Crick match to miR nucleotides 2–8, followed by an A) and "7mer-m8" sites (the Watson–Crick match to miR nucleotides 2–8) denoted in TargetScanS.

Functional Annotation Analysis. Testing for overrepresentation of functional categories was carried out using the Database for Annotation, Visualization, and Integrated Discovery (DAVID) version 2008 (18, 19). Categories analyzed included GO categories (Biological Process, Molecular Function, and Cellular Component), protein domain categories (InterPro Name, Superfamily Name, SMART Name), pathways database (KEGG Pathways), and functional categories (COG Ontology, Sp Pir Keywords, Up Seq Feature). The Benjamini correction for multiple testing was applied to the Expression Analysis Systematic Explorer (EASE) scores (20), and the significance threshold was set for an adjusted $P < 0.05$.

Expression of GAL4 Drivers

To check the expression pattern of GAL4, we used DJ715 and NP5941 lines to drive UAS-GFP. In the DJ715 line, GAL4 is reported to be expressed in the adult brain (21). We find that when used to drive UAS-GFP, this GAL4 is expressed in the larval oe-

nocytes, testes and accessory gland, salivary glands, and nervous system in addition to the adult brain (Fig. S1 *A–E*). According to the Drosophila Genomics Resource Center Web site, NP5941 (DGRC no. 113798) is reported to be expressed in larval oenocytes and adult genitalia. When using NP5941-GAL4 to drive UAS-GFP, we did observe the GFP expression in oenocytes and genitalia. We also observed NP5941-GAL4 expression in imaginal disks and salivary gland of third instar larvae as well as in adult abdomen, proboscis, antennae, leg, and wing (Fig. S1 *F–O*). The in situ hybridization of miR-311 showed ubiquitous expression in imaginal disks (all the disks of leg, wing, and eye-antenna; Richard Carthew, Northwestern University, Evanston, IL, personal communication). Our observation of larval and adult expression of NP5941-GAL4 is consistent with the results of in situ hybridization in general. In the miR collection of Ruby et al. (22), *miR310s* are detected to be expressed in embryo, imaginal disks, brains, and salivary glands from third instar larvae, adult heads, and adult bodies. The tissue distribution of *miR310s* in deep sequencing is generally concordant with the expression pattern of NP5941-GAL4. Moreover, the observed high GFP intensity in third instar larval imaginal disks, salivary gland, and brain is consistent with the relatively high level of *Dm310s* expression in the pooled imaginal disk library of deep sequencing (22). Therefore, NP5941-GAL4 expression is consistent with the results of in situ hybridization and deep sequencing, likely to mimic the expression pattern of native *miR310s*.

Overexpression of *Dm310s* and *Dp310s* Under the Control of GAL4

We performed Northern blot hybridization and semiquantitative RT-PCR to verify the overexpression of transgenic *Dm310s* and *Dp310s* under the control of GAL4 driver NP5941. Both *Dp310s* and *Dm310s* are indeed expressed in the third instar larvae when driven by GAL4 (Fig. 1 *B* and *C* and Fig. S2). We should also point out that *Dp310s* are slightly less highly expressed than *Dm310s*, despite the fact that the lethality effect is much stronger for *Dp310s*. In control larvae that do not carry the transgenic *Dp310s* or *Dm310s*, the expression of this miR was detected by RT-PCR (Fig. 1*B*) but not by Northern blot analysis (Fig. S2), which is consistent with the known expression pattern of *miR310s* by deep sequencing (22, 23). Thus, GAL4 enhances the expression of *miR310s* in the transgenic lines.

Effect of *Dps-miR-310* on WGE

Dm310s and *Dp310s* share a conserved seed, except that the seed of *Dps-miR-310* (AUUGCAG) differs from the others (AUUGCAC) at the eighth position (Fig. 1). To assess how much this change may have contributed to the observed misregulation in the *Dp310s* line, we examined the expression pattern of the putative targets of *Dps-miR-310*. In our tiling array dataset, there are 252 conserved targets of *Dps-miR-310* predicted by TargetScanFly Custom. Among them, 26 genes do not overlap with the predicted targets of *Dm310s*. The fold changes of these *Dps-miR-310*–specific targets ($n = 26$) did not significantly vary between the *Dm310s* and *Dp310s* lines ($P = 0.159$, Kruskal–Wallis test). Indeed, only 4 of the 26 *Dps-miR-310*–specific targets are significantly misexpressed in *Dp310s*. These 4 targets are also misregulated in the *Dm310s* lines. Therefore, the seed base change does not have an important role in the WGE difference between the *Dm310s* and *Dp310s* lines.

Different Strength of miRNA-Target Interactions Between *Dm310s and Dp310s*

Although seed match is crucial for target recognition, secondary structure and several features of site context may also help to specify miRNA targeting (17, 24). We have estimated the miRNA-target interaction for pairwise 3′UTR sequences of predicted targets and mature sequences of *Dm310s* and *Dp310s* by using (*i*) ΔΔG, the energy difference between miRNA-target duplex formation and unpairing, as implemented in PITA (17), and (*ii*) context score, considering features of site-type contribution, 3′ pairing contribution, local adenine-uracil (AU) contribution, and position contribution, as implemented in TargetScan (24). Among the 205 putative targets with conserved 8-mers (8-mer and 7-mer-m8 sites) match to mature *Dm310s*, 137 and 92 genes in tiling data have a more negative ΔΔG or context score for *Dm310s* than *Dp310s*, respectively. Even if these predicted targets have stronger binding affinity or more favorable sites for *Dm310s*, they were still significantly less down-regulated in the *Dm310s* line than in the *Dp310s* line (ΔΔG, $P = 3.563 \times 10^{-6}$ and context score, $P = 2.305 \times 10^{-5}$; one-sided Kolmogorov–Smirnov test). Therefore, the strong miRNA-target interaction itself cannot account for the observation that *Dp310s* are more disruptive than *Dm310s*.

1. Saitou N, Nei M (1987) The neighbor-joining method: A new method for reconstructing phylogenetic trees. *Mol Biol Evol* 4:406–425.
2. Kimura M (1980) A simple method for estimating evolutionary rates of base substitutions through comparative studies of nucleotide sequences. *J Mol Evol* 16:111–120.
3. Tamura K, Dudley J, Nei M, Kumar S (2007) MEGA4: Molecular Evolutionary Genetics Analysis (MEGA) software version 4.0. *Mol Biol Evol* 24:1596–1599.
4. Brand AH, Perrimon N (1993) Targeted gene expression as a means of altering cell fates and generating dominant phenotypes. *Development* 118:401–415.
5. Rubin GM, Spradling AC (1982) Genetic transformation of *Drosophila* with transposable element vectors. *Science* 218:348–353.
6. Zhao T, et al. (2008) A *Drosophila* gain-of-function screen for candidate genes involved in steroid-dependent neuroendocrine cell remodeling. *Genetics* 178:883–901.
7. Chen C, et al. (2005) Real-time quantification of microRNAs by stem-loop RT-PCR. *Nucleic Acids Res*, 10.1093/nar/gni178.
8. Cherbas L (2006) *Dendrimer Use and Hybridization Protocol*. (The Center for Genomics and Bioinformatics, Indiana University, Bloomington, IN) *CGB Technical Report 2006–2008*.
9. Smyth GK, Speed T (2003) Normalization of cDNA microarray data. *Methods* 31:265–273.
10. Smyth GK (2004) Linear models and empirical Bayes methods for assessing differential expression in microarray experiments. *Stat Appl Genet Mol Biol* 3:Article3.
11. Benjamini Y, Hochberg Y (1995) Controlling the false discovery rate: A practical and powerful approach to multiple testing. *J R Stat Soc B* 57:289–300.
12. Kent WJ (2002) BLAT—The BLAST-like alignment tool. *Genome Res* 12:656–664.
13. Ihaka R, Gentleman R. (1996) R: A language for data analysis and graphics. *Journal of Computational and Graphical Statistics* 5:299–314.
14. Lewis BP, Burge CB, Bartel DP (2005) Conserved seed pairing, often flanked by adenosines, indicates that thousands of human genes are microRNA targets. *Cell* 120:15–20.
15. Kheradpour P, Stark A, Roy S, Kellis M (2007) Reliable prediction of regulator targets using 12 *Drosophila* genomes. *Genome Res* 17:1919–1931.
16. Grün D, Wang YL, Langenberger D, Gunsalus KC, Rajewsky N (2005) microRNA target predictions across seven *Drosophila* species and comparison to mammalian targets. *PLOS Comput Biol* 1:e13.
17. Kertesz M, Iovino N, Unnerstall U, Gaul U, Segal E (2007) The role of site accessibility in microRNA target recognition. *Nat Genet* 39:1278–1284.
18. Dennis G, Jr, et al. (2003) DAVID: Database for annotation, visualization, and integrated discovery. *Genome Biol* 4:P3.
19. Huang W, Sherman BT, Lempicki RA (2009) Systematic and integrative analysis of large gene lists using DAVID bioinformatics resources. *Nat Protoc* 4:44–57.
20. Hosack DA, Dennis G, Jr, Sherman BT, Lane HC, Lempicki RA (2003) Identifying biological themes within lists of genes with EASE. *Genome Biol*, 10.1186/gb-2003-4-10-r70.
21. Seroude L (2004) Seroude insertions. Personal communications to FlyBase: FBrf01-78828 (http://flybase.org/reports/FBrf0178828.html).
22. Ruby JG, et al. (2007) Evolution, biogenesis, expression, and target predictions of a substantially expanded set of *Drosophila* microRNAs. *Genome Res* 17:1850–1864.
23. Chung WJ, Okamura K, Martin R, Lai EC (2008) Endogenous RNA interference provides a somatic defense against *Drosophila* transposons. *Curr Biol* 18:795–802.
24. Grimson A, et al. (2007) MicroRNA targeting specificity in mammals: Determinants beyond seed pairing. *Mol Cell* 27:91–105.

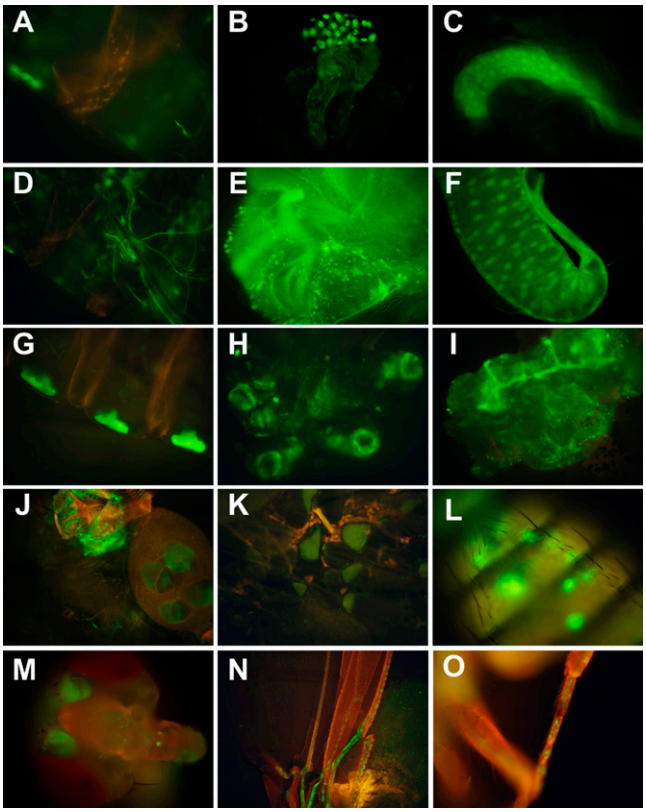

Fig. S1. Expression pattern of UAS-GFP driven by DJ715-GAL4 and NP5941-GAL4. The expression of DJ715-GAL4 was observed in oenocytes (*A*), testes and accessory gland (*B*), salivary gland (*C*), nervous system (*D*), and brain (*E*). The expression of NP5941-GAL4 was observed in salivary gland (*F*), oenocytes (*G*), imaginal disks (*H*), brain (*I*), female genitalia (*J*), ovaries (*K*), abdomen (*L*), proboscis and antennae (*M*), wing (*N*), and leg (*O*).

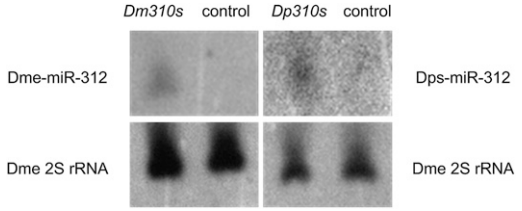

Fig. S2. Overexpression of *Dm310s* and *Dp310s* as detected by Northern blot hybridization. (*Lower*) 2S rRNA is shown as a loading control. (*Upper Left*) Control and *NP5941-GAL4/UAS-Dm310s* carrying larval RNA probed with a digoxigenin-labeled probe antisense to Dme-miR-312 are shown. (*Upper Right*) Control and *NP5941-GAL4/UAS-Dp310s* carrying larval RNA probed with a digoxigenin-labeled probe antisense to the second *D. pseudoobscura* miR encoded in the cluster are shown.

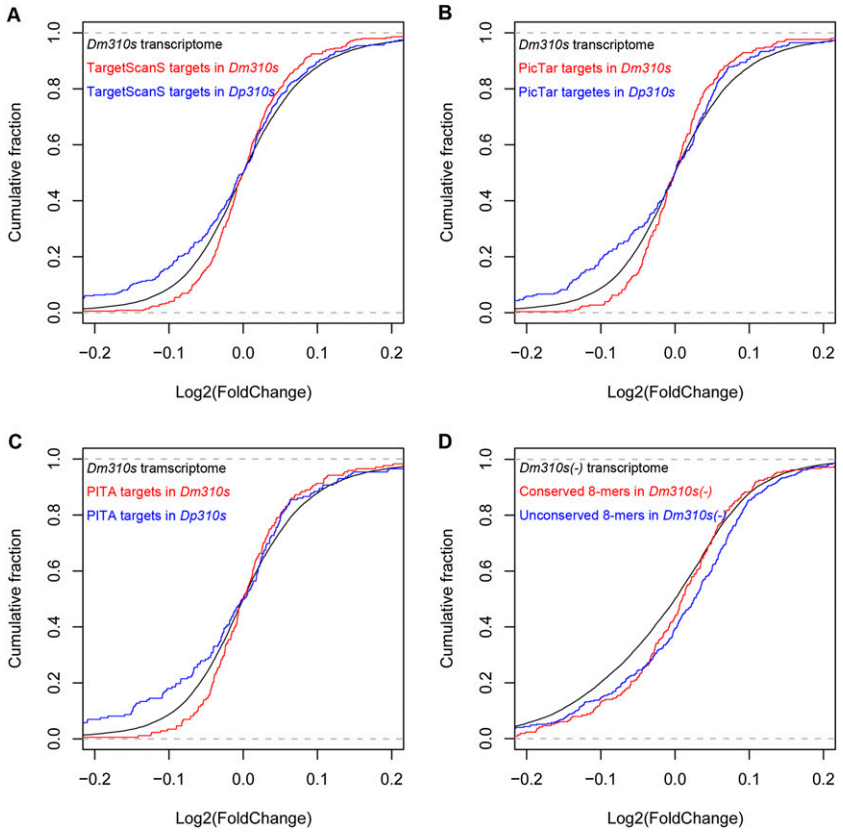

Fig. S3. Effects of the transgenic *miR310s* on the predicted target genes. The putative targets predicted by TargetScanS ($n = 346$) (*A*), PicTar ($n = 255$) (*B*), and PITA TOP category ($n = 172$) (*C*) tended to be more down-regulated in *Dp310s* (blue curves) than in *Dm310s* (red curves) lines ($P = 2.98 \times 10^{-4}$, $P = 2.98 \times 10^{-4}$, and $P = 7.53 \times 10^{-3}$ for TargetScanS, PicTar, and PITA TOP category targets, respectively, by Kolmogorov–Smirnov test). (*D*) In the *Dm310s*(–) line, the putative targets with conserved and unconserved 8-mer sites were overexpressed relative to the transcriptome as a whole when *miR310s* were deleted (plotted as in Fig. 3*D*.)

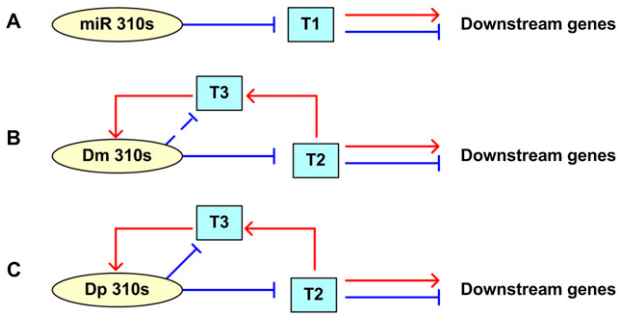

Fig. S4. Motifs that regulate the expression of direct targets (T1–T3) of *miR310s*. (*A*) Simple repression. An example of T1 may be *CrebA*, which is down-regulated in both *Dm310s* and *Dp310s* lines. (*B*) Feedback loop. The simple mechanism might account for the unchanged expression of the direct target in *Dm310s* lines (T2), an example of which is *Ras85D*. (*C*) Feedback loop interrupted. T2 in *Dp310s* lines was down-regulated, suggesting interruption of the feedback loop. We are in the process of identifying possible candidates for T3 when T2 is *Ras85D*. One of the candidates is the Δ transcript, which is a target of *Dp310s* as predicted by PITA [Kertesz M, Iovino N, Unnerstall U, Gaul U, Segal E (2007) The role of site accessibility in microRNA target recognition. *Nat Genet* 39:1278–1284].

Other Supporting Information Files

Table S1 (DOC)
Table S2 (DOC)